Electronic Supplementary Material (ESI) for Physical Chemistry Chemical Physics.

Supplementary Materials

2D antiferromagnetic semiconducting FeCN with interesting properties

Zhicui Wang[1†], Huan Lou[1,2†], Xu Yan[1], Yong Liu[1*], and Guochun Yang[1*]

[1]*State Key Laboratory of Metastable Materials Science & Technology and Key Laboratory for Microstructural Material Physics of Hebei Province, School of Science, Yanshan University, Qinhuangdao 066004, China*

[2]*Department of Physics, College of Science, Jiangsu University of Science and Technology, Zhenjiang 212003, People's Republic of China*

[†]Zhi-Cui Wang and Huan Lou contributed equally to this work.

*Corresponding Authors E-mail:yongliu@ysu.edu.cn; yanggc@ysu.edu.cn.

Index **page**

Computational Details

Our structural prediction approach is based on a global minimization of free energy surfaces merging ab initio total-energy calculations with CALYPSO (Crystal structure AnaLYsis by Particle Swarm Optimization) methodology as implemented in the CALYPSO code [1,2]. The structures of stoichiometry FeCN monolayer were searched with simulation cell sizes of 1-4 formula units (f.u.). In the first step, random structures with certain symmetry are constructed in which atomic coordinates are generated by the crystallographic symmetry operations. Local optimizations [3] using the VASP code were done with the conjugate gradients method and stopped when energy changes became smaller than 1×10^{-5} eV per cell. After processing the first-generation structures, 60% of them with lower Gibbs free energies are selected to construct the next generation structures by PSO (Particle Swarm Optimization). 40% of the structures in the new generation are randomly generated. A structure fingerprinting technique of bond characterization matrix is applied to the generated structures, so that identical structures are strictly forbidden. These procedures significantly enhance the diversity of the structures, which is crucial for structural global search efficiency. In most cases, structural searching simulations for each calculation were stopped after generating 1000 ~ 1200 structures (e.g., about 20 ~ 30 generations).

To further analyze the structures with higher accuracy, we select a number of structures with lower energies and perform structural optimization using density functional theory within the generalized gradient approximation [4] as implemented in the VASP code. The cut-off energy for the expansion of wavefunctions into plane waves is set to 500 eV in all calculations, and the Monkhorst–Pack k-mesh with a maximum spacing of $2\pi \times 0.03$ Å^{-1} was individually adjusted in reciprocal space with respect to the size of each computational cell. This usually gives total energies well converged within ~1 meV/atom. The electron-ion interaction was described by using all-electron projector augmented-wave method (PAW) with $3d^7 4s^1$, $2s^2 2p^3$, and $2s^2 2p^2$ considered as valence electrons for Fe, C, and N atoms, respectively. The cohesive energy E_{coh} is calculated according to the equation below:

$$E_{coh} = \left(4E_{Fe} + 4E_C + 4E_N - E_{FeCN}\right)/12 \quad (1)$$

where E_{Fe}, E_C, E_N, and E_{FeCN} are the energies of the Fe, C, and N atoms, as well as the FeCN unit cell, respectively.

In this paper, the U = 4.0 eV value of DFT+U is calculated based on the linear response approximation method [4]. As shown below [Fig. S1], we calculate a series of different additional potentials. The non-self-consistent and the self-consistent response functions are found from a linear fit of the number of *d*-electrons as a function of the additional potential V.

Then we get:

$$U = \chi^{-1} - \chi_0^{-1} \approx \left(\frac{\partial N^{SCF}}{\partial V}\right)^{-1} - \left(\frac{\partial N^{NSCF}}{\partial V}\right)^{-1} = \left(\frac{1}{0.2}\right)^{-1} - \left(\frac{1}{1.5}\right)^{-1} = 4.3\,\text{eV} \tag{2}$$

we have calculated the T_N of the FeCN as estimated from the Hamiltonian equation:

$$H = -\sum_{\langle ij\rangle} J_1 S_i S_j - \sum_{\langle ik\rangle} J_2 S_i S_k - \sum_{\langle il\rangle} J_3 S_i S_l - \sum_{\langle i\rangle} S_i A_{ii} S_i \tag{3}$$

The magnetic moment of Fe atoms versus temperature was calculated using the open-source software MCSOLVER and Monte Carlo (MC) simulation method [5].

Supplementary Figures

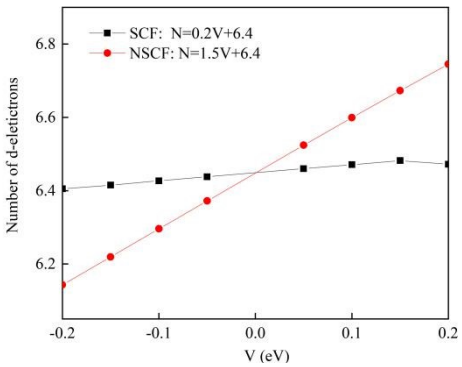

Fig. S1 Linear response of the number of *d*-electrons on Fe atomic site as a function of the additional potential V.

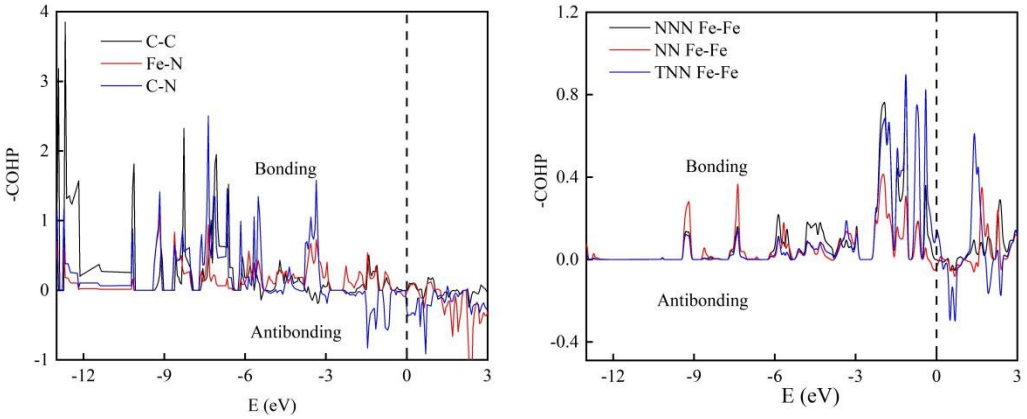

Fig. S2 The negative crystal orbital Hamilton population (-COHP) values of C-C, Fe-N, C-N and Fe-Fe bonds of the FeCN monolayer.

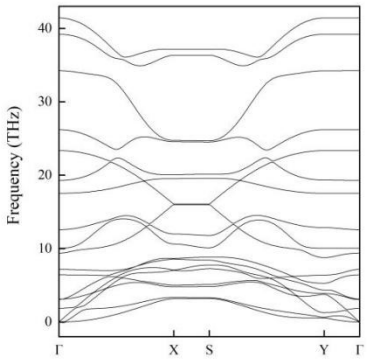

Fig. S3 Phonon dispersion curve of the FeCN monolayer at 300 K.

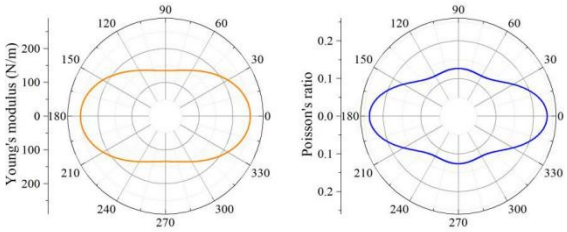

Fig. S4 The Young's modulus $E(\theta)$ (left) and Poisson's ratio v (θ) (right) of the FeCN monolayer.

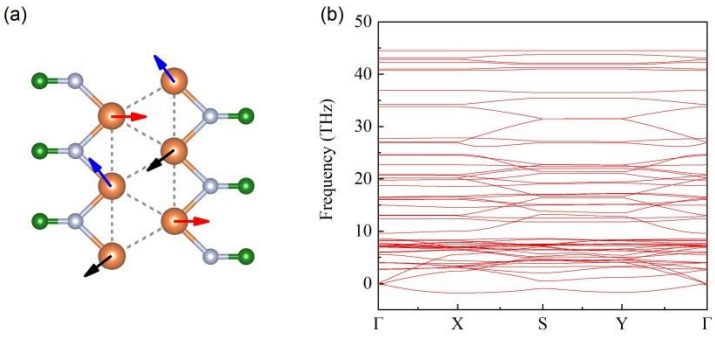

Fig S5 (a) Nonlinear AFM configuration of the FeCN monolayer. (b) Phonon dispersion curve of the FeCN monolayer in nonlinear AFM configuration.

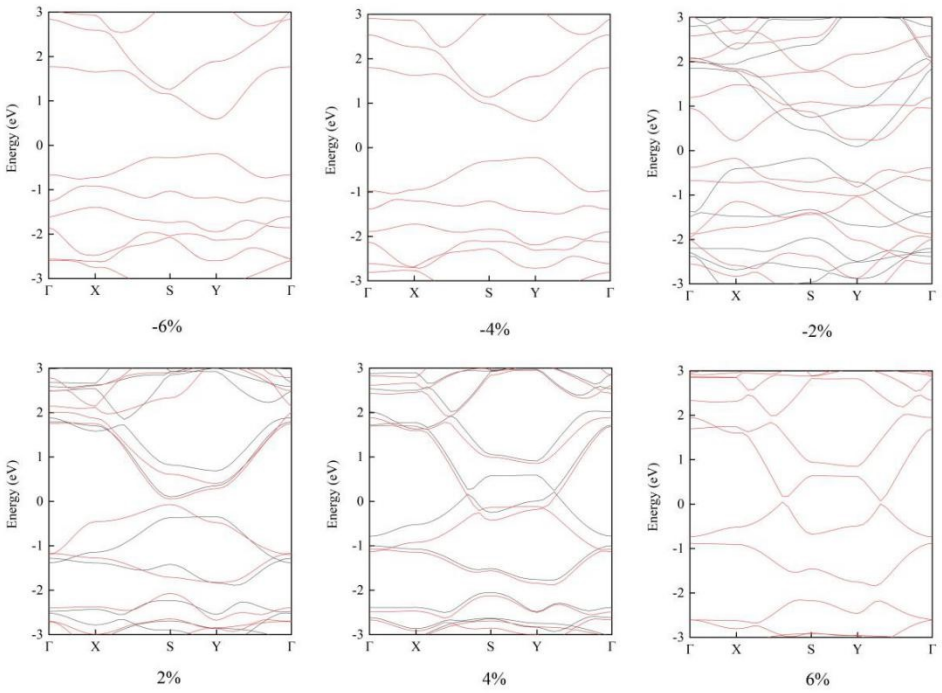

Fig. S6 The calculated band structures under biaxial strain (-6% to 6%) of the FeCN monolayer using HSE06.

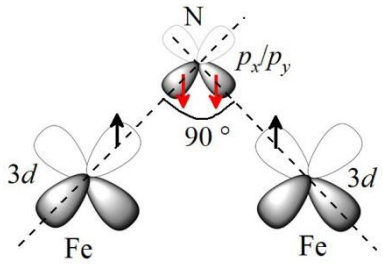

Fig. S7 Schematic illustration of the mechanism of the super-exchange interaction (Fe-N-Fe).

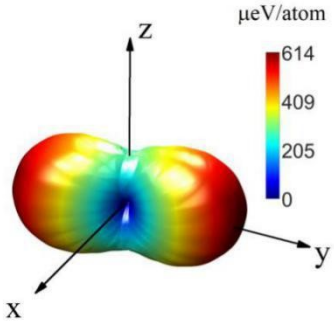

Fig. S8 Three-dimensional MAE of the FeCN monolayer.

Supplementary Tables

Table S1. The bond length and bond angle in the FeCN monolayer.

C-C bond (Å)	C-N bond (Å)	Fe-N bond (Å)	Fe-Fe bond (Å)	Fe-Fe bond (Å)	Fe-N-Fe Angle θ (°)
1.49	1.32	1.85(1.86)	2.59	2.67(2.64)	88.38

Table S2. Structural information of the predicted FeCN monolayer.

Phase	Space Group	Lattice Parameters (Å,°)	Atoms	Atomic Positions (fractional) *x*	*y*	*z*
FeCN	*P*-1	*x*= 8.36	Fe1	0.64	0.37	0.50
		y= 5.18	Fe2	0.36	0.13	0.50
		z= 12.63	Fe3	0.64	0.87	0.50
		a= 90.75	Fe4	0.36	0.63	0.50
		β= 94.73	N1	0.20	0.38	0.50
		γ= 90.02	N2	0.80	0.12	0.50
			N3	0.20	0.88	0.50
			N4	0.80	0.62	0.50
			C1	0.96	0.12	0.50
			C2	0.04	0.38	0.50

C3	0.96	0.62	0.50
C4	0.04	0.88	0.50

Table S3. The total energies in the considered different magnetic configurations.

FM (eV)	AFM1 (eV)	AFM2 (eV)	AFM3 (eV)
-87.011	-87.075	-87.849	-87.813

References

[1] Y. Wang, J. Lv, L. Zhu and Y. Ma, Phys. Rev. B 82 (2010) 094116.

[2] Y. Wang, J. Lv, L. Zhu and Y. Ma, Comput. Phys. Commun. 183 (2012) 2063.

[3] G. Kresse and J. Furthmüller, Phys. Rev. B 54 (1996) 11169.

[4] Matteo Cococcioni and Stefano de Gironcoli, Phys. Rev. B 71 (2005) 035105.

[5] A. Bafekry, C. Stampfl, B. Akgenc, and M. Ghergherehchi. Phys. Chem. Chem. Phys. 4 (2022) 22.